



## Nano-Structural Analysis of a Lyotropic Liquid Crystal (TTAB + water + decanol ternary) System by Salt ( $\text{NH}_4\text{Br}$ ) Addition

Ozgur Masalci, Nadide Kazanci, Ilghar Orujalipoor & Semra İde

**To cite this article:** Ozgur Masalci, Nadide Kazanci, Ilghar Orujalipoor & Semra İde (2015) Nano-Structural Analysis of a Lyotropic Liquid Crystal (TTAB + water + decanol ternary) System by Salt ( $\text{NH}_4\text{Br}$ ) Addition, *Molecular Crystals and Liquid Crystals*, 609:1, 70-79, DOI: 10.1080/15421406.2014.957476

**To link to this article:** <http://dx.doi.org/10.1080/15421406.2014.957476>



Published online: 11 Apr 2015.



Submit your article to this journal [↗](#)



Article views: 58



View related articles [↗](#)



View Crossmark data [↗](#)

# Nano-Structural Analysis of a Lyotropic Liquid Crystal (TTAB + water + decanol ternary) System by Salt ( $\text{NH}_4\text{Br}$ ) Addition

OZGUR MASALCI,<sup>1,\*</sup> NADIDE KAZANCI,<sup>1</sup> ILGHAR ORUJALIPOOR,<sup>2</sup> AND SEMRA İDE<sup>3</sup>

<sup>1</sup>Department of Physics, Ege University, Bornova, Izmir, Turkey

<sup>2</sup>Department of Nanotechnology and Nanoscience, Hacettepe University, Beytepe, Ankara, Turkey

<sup>3</sup>Department of Physics Engineering, Hacettepe University, Beytepe, Ankara, Turkey

*In the present study, the ionic effect of salt addition to a lyotropic liquid crystal (LLC) system was investigated.  $\text{NH}_4\text{Br}$  salt was added to TTAB + water + decanol ternary system and the structural changes in lyotropic phases were characterized. First, phase transitions were illustrated by polarized microscope and secondary, small-angle x-ray scattering was used as an analytical method to determine the nano-structured mesophases of the newly prepared liquid crystal samples. The expected fibrous structures were characterized by the form factor of polydisperse oblate ellipsoids. The self-assembled networks related with these ellipsoids were also explained with hexagonal, distorted hexagonal, and lamellar formations.*

**Keywords** Liquid crystals; optical microscopy; phase transitions; small-angle scattering

## 1. Introduction

The self-association process of amphiphilic molecules into micelles, vesicles, or membranes tend to play an important part in a range of fields from biological systems to technical applications [1]. The establishment of essential structural parameters of surfactant self-aggregation is needed to comprehend physical mechanisms to drive the formation of their molecular assemblies in solution just as in their uses to form lyotropic liquid crystal (LLC) [2].

Surfactant self-assembly accounts for a variety of different structures. Amphiphile-containing systems are best classified into homogeneous or single phase systems and heterogeneous systems with two or more phases [3]. Surfactant molecules over the critical micellar concentration (cmc) in solution form micelles. The aggregate morphology includes a great variety of shapes and sizes [4]. Micelle morphology caused by the surfactant is

---

\*Address correspondence to Ozgur Masalci, Ege University, Faculty of Science, Department of Physics, Bornova, Izmir, Turkey. E-mail: ozgur.masalci@ege.edu.tr

Color versions of one or more of the figures in the article can be found online at [www.tandfonline.com/gmcl](http://www.tandfonline.com/gmcl).

influenced by concentration changes [5,6], headgroup area [7,8], charge density [9], and electrostatic interactions among the head groups [10–13]. Bilayer, cylindrical, and spherical self-assembled structures are usually defined by a surfactant packing parameter,

$$P = V/a_0l, \quad (1)$$

where  $V$  is the surfactant chain volume,  $a_0$  is the effective hydrophobic/hydrophilic interfacial area, and  $l$  is the chain length. Based upon the above plan, ideal bilayer, bi-continuous, cylindrical, and spherical geometries have  $P$  values as 1, 2/3, 1/2, and 1/3, respectively [4,14,15].

Addition of ions to an aqueous micellar amphiphile solution acts through two mechanisms in principle [16]. The tendency of the added ions toward intense hydration decreases the quantity of “free water” necessary for head parts to be solved at the aggregate surface. The electrostatic properties of the added ions change the dielectric features of the isotropic solvent and therefore the repulsion interaction between equally charged aggregates in addition to the electrostatic repulsion between the adjacent head groups at the micelle surface. Both mechanisms contain a wide range of enthalpic and entropic contributions, which make it hard to pre-estimate the net salt effect or at least the dominant salt effect in a given system [17].

The study chose TTAB, one of cationic surfactants, which has additional advantages as compared with other surfactants and is of antibacterial quality and surface activity [18]. These are used as cationic softeners, lubricants, retarding agents, and antistatic agents. TTAB + water + decanol ternary system was previously studied with the result that lyotropic mesophases were determined [19].

Complex polymorphism of ternary systems, comprising an amphiphile /water/alcohol and/or salt has been extensively studied over the last two decades [20]. Since interfaces between polar and apolar groups of amphiphilic matters have a tendency to a spontaneous combination, there emerge numerous polymorphisms of various forms and symmetries [20]. Hydrophilic interactions between hydrophobic and head groups on hydrocarbon–water interface are essential driving forces turning amphiphiles into groupings.

The present study added the salt of  $\text{NH}_4\text{Br}$  into the samples of hexagonal property in the predetermined ternary system. Presence of  $\text{NH}_4\text{Br}$  in the solution affects electrical atmosphere of the medium, which can lead to various changes in the lyotropic structures. Then we examined using polarized optic microscope (POM) and small-angle x-ray scattering (SAXS). The study enables us to better understand inter- and intra-micellary interactions in a solution of cationic surfactants and their organized mesophases. Thereby, simple ionic LLC systems such as the one being studied here could be quite beneficial as a model system for more general understanding of ionic effects in soft matter in biological systems such as membranes.

## 2. Materials and Methods

### 2.1. Sample Preparation

TTAB (cat. No. T-4762) and ammonium bromide were obtained from Sigma and Fuluka (cat No. 09715) and used without further purification. Ultrapure water was used as a solvent. The required amount of components has been weighed by an And HR-120 scale with an accuracy of  $10^{-4}$  g. The mixtures preserved in hermetically closed vessels have been stored for homogenization in a Memmert 400 thermostat at  $323 \pm 0.1$  K.

According to the phases diagram determined in our previous study, weight ratio of TTAB:decanol:water is fixed as 40:1:59, which presents sample hexagonal E mesophase, which remains unchanged with the addition of salt ( $\text{NH}_4\text{Br}$ ) of 1, 2, and 3% in weight.

## 2.2. Polarized Optical Microscopy (POM) Measurement

Homogeneous lyotropic systems were examined using polarized light microscope. Texture types of lyotropic phases were identified by Olympus BX-P POM, Olympus SC35 microphotographic system, and a special stage.

## 2.3. Small Angle X-ray Scattering (SAXS)

Small angle x-ray scattering measurements of LLC samples were performed in HECUS System 3 with a Kratky optic, micro-line collimation and position-sensitive line detectors at 50 kV–50 mA. A conventional x-ray source ( $\text{CuK}_\alpha$ ,  $\lambda = 0.154$  nm) and ISO-DEBYEFLEX 3003 generator were used during the scattering measurements given by  $I(q) - q$ , where  $I$  is the scattered intensity, and  $q$  is the magnitude of scattering vector. Temperature and exposure time of each sample were 23°C and 700 s, respectively.

# 3. Result and Discussion

## 3.1. Characterization of Nano-aggregations

Phase changes is one of the significant physical phenomena to govern morphology of heterogeneous structures [21]. Based on variation in concentration, lyotropic phases may transform into one another [22–24]. Amphiphilic aggregates combined to make free energy minimum form many new mesophases, which consist of electrostatic and repulsive forces as basic interactions. Addition of salt to LLC phase has been found to change phase transition properties, and thus orientational order as well as thermal stability [17]. Emphasis is paid to the addition of salt to LLC phase since it enables a better understanding of nature and role of electrostatic interactions within the complicated structure of a soft material.

Birefringence textural morphologies are important as the current knowledge of the molecular arrangement as a proven standardized method for the characterization of different phases of liquid crystals [25,26].

The positions and orientations of nano-structured aggregations can align themselves with respect to each other. Interactions between the aggregations lead short-range order and cause an increased probability to find next neighbor aggregation at a specific distance.

The narrow and intensive peaks with well-defined  $q$  values and the ratios of the peak positions can be also detected in SAXS profiles, when the positions of nano-aggregations become more ordered in long range. The evidences of these short- and long-range orders in the studied samples can be obtained by the positional orders (1, 2, 3... for lamellar, and 1,  $\sqrt{3}$ , 2... for hexagonal symmetries) in the perfect crystalline samples. For example:  $q_2/q_1 = 2$  indicates lamellar order.

Lamellar and hexagonal phases were obtained from characteristic  $q$  positions which have diffraction peaks related with these liquid crystalline structures. Figure 1 illustrates SAXS patterns, including all phases. Vertical and horizontal axes are related with scattering intensity in log scale and magnitude of scattering vector ( $q$ ), respectively.

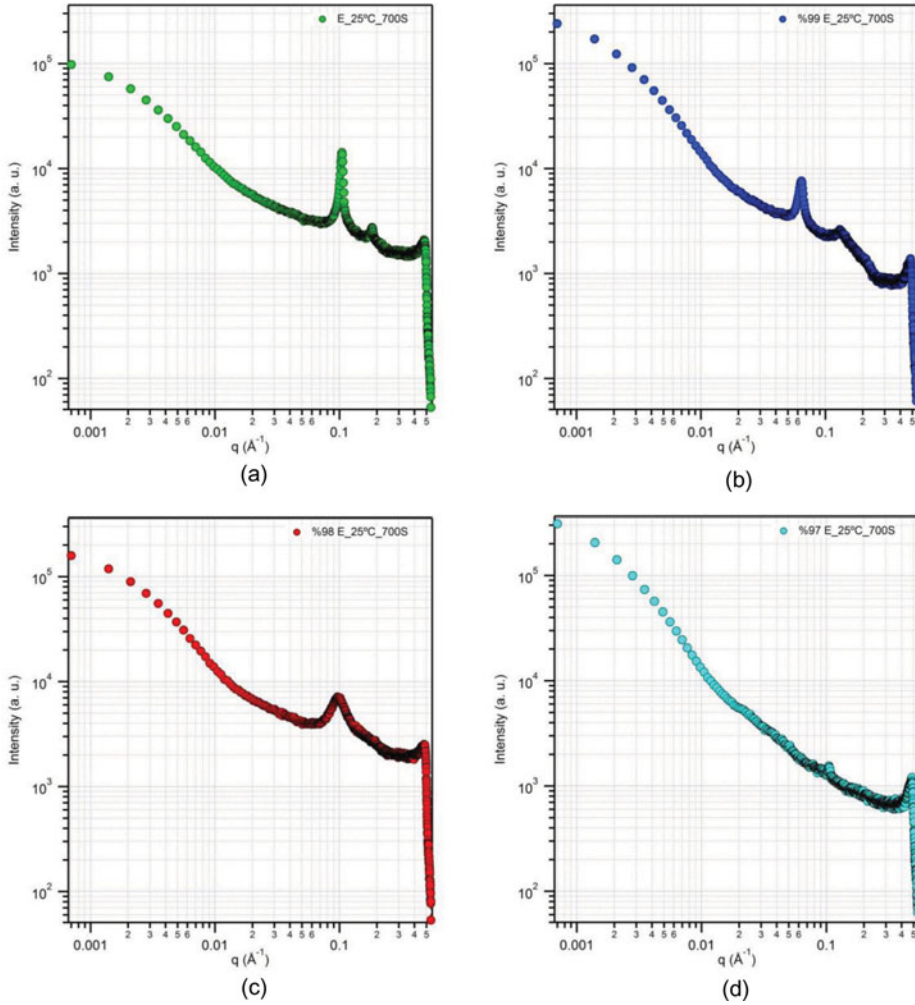


**Figure 1.** SAXS profiles of the samples (a) 100% E phase: control sample, (b) 99% E + 1%  $\text{NH}_4\text{Br}$ , (c) 98% E + 2%  $\text{NH}_4\text{Br}$ , and (d) 97% E + 3%  $\text{NH}_4\text{Br}$ .

The following form factor  $[P(q)]$  equation was used for poly disperse oblate ellipsoid model, which is well fitted to scattering data of 99% E + 1%  $\text{NH}_4\text{Br}$  and 98% E + 2%  $\text{NH}_4\text{Br}$  [27,28]:

$$P(q) = \frac{\text{Scale}}{V_{\text{ell}}} (\rho_{\text{ell}} - \rho_{\text{solv}})^2 \int_0^{\infty} f^2[qr(1 + x^2(v^2 - 1))^{1/2}] dx + bkg, \quad (2)$$

where

$$f(z) = 3V_{\text{ell}} \frac{(\sin z - z \cos z)}{z^3}, \quad v = \frac{R_a}{R_b}, \quad (3)$$

**Table 1.** Details of diffraction peaks indicating different phases and phase transitions

100% E phase	99% E + 1% NH <sub>4</sub> Br	98% E + 2% NH <sub>4</sub> Br	97% E + 3% NH <sub>4</sub> Br
Hexagonal	Hexagonal → Distorted hexagonal	Distorted hex. → Distorted lamellar	Distorted lamellar
Lattice spacing 68.81 Å	Lattice spacing 96.73 Å	Lattice spacing 63.36 Å	Lattice spacing 59.58 Å
<b>Peak 1</b> $q = 0.119 \text{ Å}^{-1}$ $d_1 = 59.58 \text{ Å}$ ( $q = 2\pi/d$ )	<b>Peak 1</b> $q = 0.065 \text{ Å}^{-1}$ $d_1 = 96.73 \text{ Å}$	<b>Peak 1</b> $q = 0.099 \text{ Å}^{-1}$ $d_1 = 63.36 \text{ Å}$	<b>Peak 1</b> $q = 0.105 \text{ Å}^{-1}$ $d_1 = 59.58 \text{ Å}$
<b>Peak 2</b> $q = 0.184 \text{ Å}^{-1}$ $d_2 = 34.10 \text{ Å}$ $q_2/q_1 \sim \sqrt{3}$	<b>Peak 2</b> $q = 0.132 \text{ Å}^{-1}$ $d_2 = 47.61 \text{ Å}$	<b>Peak 2</b> (disappeared)	

$V$  = volume; and  $\rho$  = electron densities of ellipsoid or solvent. If the scale is equal to the particle volume fraction,  $f$ , then the returned value is the scattered intensity per unit volume,  $I(q) = f \cdot P(q)$ .

### 3.2. SAXS and POM Results

Data analysis was based on crystallographic peaks (Fig. 1) and fitting the scattering curve to ellipsoid model defined by the above-mentioned form factors. First characteristic results of the studied samples were briefly given in Table 1.

Initial examination of the texture of ternary system comprising 40% TTAB + 59% water + 1% decanol without salt (control sample) showed the two-dimensional hexagonal E mesophase. Microscopic representation and structural parameters of this phase are given in Fig. 2a and Table 1 (first column).

Besides the characteristic and crystallographic peaks, the other data were also investigated to reach the shape and ordering of the nano-structured formations. For this purpose, the scattering data of 99% E + 1% NH<sub>4</sub>Br and 98% E + 2% NH<sub>4</sub>Br were focused. Fitting curves determined by IGOR Pro 6 [28] and SAXS data are presented in Fig. 3.

After the fitting process, the structural parameters were used to construct the models as seen in Table 2. Square root of [ $\chi^2$ /number of fitted data points] was between acceptable value (between 1 and 3) for the refinements of structural parameters.

Stick-shaped micelles form a hexagonal network in E mesophase, in which they are separated from each other by water and of infinite length and the same diameter [29]. Polar parts of amphiphile molecules are involved by polar sections of solvent in micelles, whereas their non-polar parts are centrally inward and can only be in touch with non-polar solvent. Hexagonal E mesophase is optically uniaxial and the optical axis is parallel to the long axis of micelles [30]. In the ternary system of TTAB + water + decanol, E mesophase exhibited a fibrous texture, which has large areas of planar orientation and typical of E mesophase [19]. The texture was found to be blinking in light when the microscope plane was rotated, which is caused by planar direction of the texture. That is, optical axis is parallel to the long axis of micelles [31].

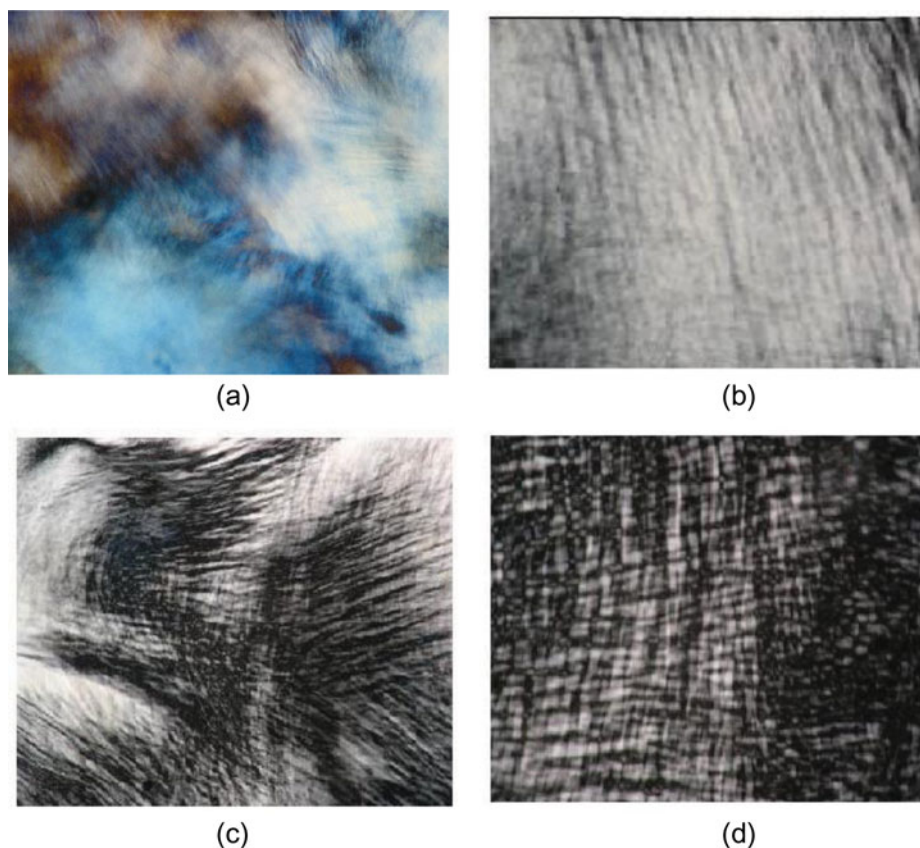


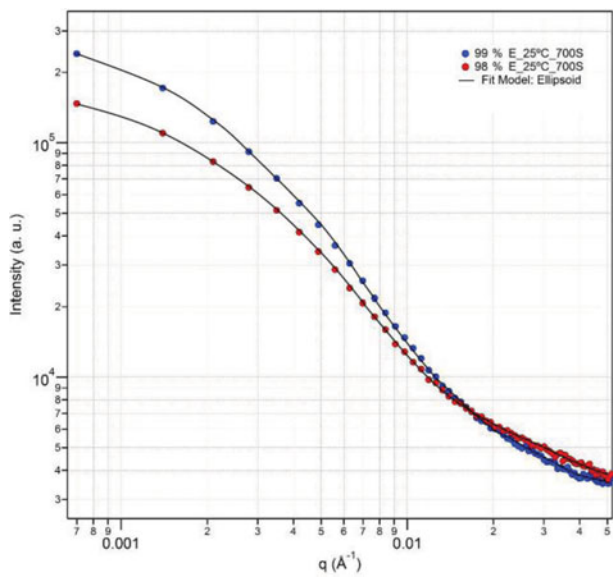
**Figure 2.** Microscopic illustrations of samples (a) Control sample (100% E phase), (b) 99% E + 1%  $\text{NH}_4\text{Br}$ , (c) 98% E + 2%  $\text{NH}_4\text{Br}$ , and (d) 97% E + 3%  $\text{NH}_4\text{Br}$ .

Addition of 1%  $\text{NH}_4\text{Br}$  in weight to the system changes the hexagonal structure and SAXS results and the texture photographs showing striped texture and distorted hexagonal phase as seen in Fig. 2b and Table 1. The striped texture is also observed to be blinking in irregular dark and bright ribbons in Fig. 2b when the microscopic plane has been rotated.

Figures 4 and 5 were obtained by using structural parameters (given in Table 1) and two programs for SAXS analysis [28,32]. In these figures, PDD is a pair distance distribution of ellipsoid formations, and the right top view in the figure is related with the structural model, which was refined by the scattering data.

The texture in Fig. 2c has been observed to appear with the addition of 2% salt. Stripe-like formations continued with decreased dimensions. Moreover, new areas of planar orientations began to appear again. With the ratio of salt increasing to 3%  $\text{NH}_4\text{Br}$  (Fig. 2d), dark stripes emerged from certain points as continuum of flaky-like structure broke down. Dark stripes are the areas where light of direction vector of liquid crystal upon sample is perpendicular to the polarization surface. Dots from which lines originated are called singular points [19].

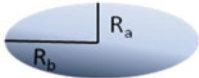
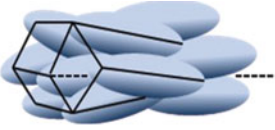
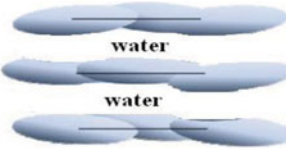
Experiments have shown that electrolytes play an important role in the mechanism of particularly ionic amphiphiles in self-assembly. It is essential for electrostatic repulsion to be screened between head groups of equivalent charges on aggregate surface for aggregation,



**Figure 3.** SAXS data (red and blue dots) and fitting curves (black lines) of two focused phases.

which is formed by hydration spheres around every head group and present counter ions. With the addition of electrolytes to the medium, screening of repulsion between head groups on aggregate surface causes micelle growth [4]. Addition of salt screens repulsion between adjacent cationic head groups and decreases their effective dimensions with the result that plate-like micelles are stimulated to grow and develop.

**Table 2.** Fit results related to SAXS analysis

Samples	1% NH <sub>4</sub> Br	2% NH <sub>4</sub> Br
Scale	1.63	1.13
R <sub>a</sub> (Å)	23.20	15.69
R <sub>b</sub> (Å)	690.12	580.25
SLD ellipsoid (Å <sup>-2</sup> )	6.98 × 10 <sup>-6</sup>	6.46 × 10 <sup>-6</sup>
SLD solvent (Å <sup>-2</sup> )	6.70 × 10 <sup>-7</sup>	6.64 × 10 <sup>-7</sup>
Incoh. BKG	125.10	120.54
Representative	model	
		
Ellipsoid	Distorted hexagonal formation along central axis indicated by discrete lines	Distorted lamellar



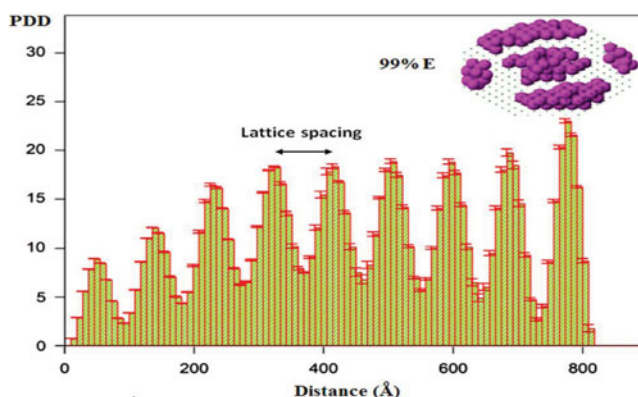


**Figure 4.** Distorted hexagonal formation [32] in the structure of 99% E + 1%  $\text{NH}_4\text{Br}$  and PDD of nano-ellipsoids after the fitting process [28].

SAXS analyses and POM observations show that addition of salt ( $\text{NH}_4\text{Br}$ ) caused hexagonal E to pass to lamellar phase. Little addition of salt enabled hexagonal E to pass to lamellar phase, which is attributed to the fact that the presence of salt ions facilitated aggregate curve in E phase to decrease [33,34]. The fact is, the more the ratio of salt, the less the repeated  $d$  distance (Fig. 6), which means that  $\text{NH}_4\text{Br}$  molecules adjacent to aggregate interface penetrate head groups of TTAB molecules, which further implies that water molecules among hydrophilic head groups decreased as well [34]. The penetration of molecules also causes the less long-range order, the deviation from more ordered stacking, and the less intensive crystalline peaks as seen in Fig. 1.

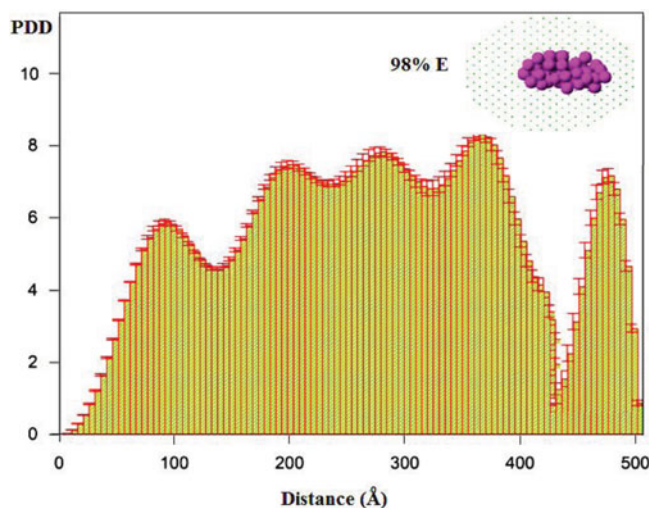


**Figure 5.** Distorted lamellar ordering in PDD of ellipsoids formation modeling by a group of pink residue balls.

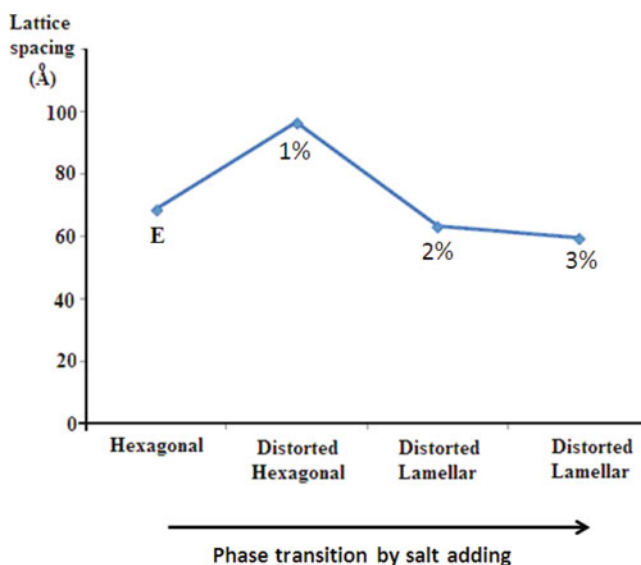


**Figure 6.** Change in lattice spacing is related with adding of salt ( $\text{NH}_4\text{Br}$ ) to LLC system.

#### 4. Conclusions

The present study has examined changes emerging with the addition of salt to the ternary system, using POM and SAXS methods. Addition of  $\text{NH}_4\text{Br}$  salt to TTAB + water + decanol ternary system has resulted in interphase transition with new mesophases. Sample of reference without any salts has exhibited a hexagonal mesophase. With the addition of 1%  $\text{NH}_4\text{Br}$  to the system, sensitive equilibrium has been upset between molecules and the system has passed to a distorted hexagonal mesophase. Increase of salt ratio to 2% and 3% has changed the hexagonal structure into a distorted lamellar mesophase, which has pointed out that the salt could act as a co-surfactant [35]. Addition of salt to the ternary system has varied the value of lattice spacing. The higher the salt, the greater the amount of ions in the system is with the result that two influences appear: (a) hydration of added ions causes free water amount to decrease; and (b) repulsive forces inside and outside the aggregate are screened [17].  $\text{NH}_4\text{Br}$  molecules have penetrated into polar head groups of TTAB molecules. Therefore, the area of effective head group ( $a_o$ ) has decreased according to Equation (1) while packing parameter ( $P$ ) has increased in ratio inverse to this area. The higher the value of  $P$ , the lesser the curvature of the structure has been with its transition to lamellar structure emergence. Accordingly, one can conclude the following: Electrostatic repulsion between cationic head groups of the surfactant and force of hydration could be changed by a small effect. The equilibrium between both forces could determine aggregation of molecules to lead to new mesophase formations.

#### References

- [1] Perger, T. M., & Bešter-Rogac, M. (2007). *J. Coll. Interface Sci.*, 313, 288–295.
- [2] Bauer, C., Bauduin, P., Girard, L., Diat, O., & Zemb, T. (2012). *Colloid Surf. Physicochem. Eng. Aspects*, 413, 92–100.
- [3] Jönsson, B., Lindman, B., Holmberg, K., & Kronberg, B. (1999). *Surfactant and Polymers in Aqueous Solution*, John Wiley: Chichester, UK.

- [4] Israellevichelli, J. N. (1992). *Intermolecular and Surface Forces*, Academic Press: London, UK.
- [5] Kroke, P. J., Magid, L. J., & Gee, J. C. (1996). *Langmuir*, 12, 699–705.
- [6] Carver M. et al. (1996). *Langmuir*, 12, 691–698.
- [7] Magid, L. J. (1998). *J. Phys. Chem. B.*, 102, 4064–4074.
- [8] Bachofer, S. J., Simonis, U., & Nowicki, T. A. (1991). *J. Phys. Chem.*, 95, 480–488.
- [9] Magid, L. J. et al. (1997). *J. Phys Chem. B.*, 101, 7919–7927.
- [10] Buwalda, R. T., Stuart, M. C. A., & Engberts, J. B. F. N. (2000). *Langmuir*, 16, 6780–6786.
- [11] Abdel-Rahem, R., Gradzielski, M., & Hoffmann, H. (2005). *J. Colloid Interface Sci.*, 288, 570.
- [12] Landázuri, G. et al. (2012). *J. Colloid. Interface Sci.*, 370, 86–93.
- [13] Zhao, Y., Yue, X., Wang, X., & Chen, X. (2013). *J. Colloid. Interface Sci.*, 389, 199–205.
- [14] Han, L., Miyasaka, K., Terasaki, O., & Che, S. (2011). *J. Am. Chem. Soc.*, 133, 11524–11533.
- [15] Manohar, C., & Narayanan, J. (2012). *Colloid. Surf. Physicochem. Eng. Aspects*, 403, 129–132.
- [16] Sein, A., & Engberts, J. B. F. N. (1995). *Langmuir*, 11, 455–465.
- [17] Dawin, U. C., Lagerwall, J. P. F., & Giesselmann, F. (2009). *J. Phys. Chem. B.*, 113, 11414–11420.
- [18] Varade, D. et al. (2005). *Colloid. Surf. A.*, 259, 95–101.
- [19] Masalci, O., & Kazanci, N. (2009). *J. Mol. Struct.*, 919, 1–6.
- [20] Amaral, L. Q. (2002). *Braz. J. Phys.*, 32, 540–547.
- [21] Iwashita, Y., & Tanaka, H. (2006). *Nature Mater.*, 5, 147–152.
- [22] Beica, T. et al. (2004). *Liq. Crystals*, 31, 325–332.
- [23] Albayrak, C., Özkan, N., & Dag, Ö. (2011). *Langmuir*, 27, 870–873.
- [24] Dong, R., & Hao, J. C. (2010). *Chem. Rev.*, 110, 4978–5022.
- [25] Burducea, G. (2004). *Rom. Rep. Phys.*, 56, 66–86.
- [26] Muniandy, G. S. V., Kan, C. S., Lim, S. C., & Radiman, S. (2003). *Physica A.*, 323, 107–123.
- [27] Feigin, L. A., & Svergun, D. I. (1987). *Structure Analysis by Small-Angle X-Ray and Neutron Scattering*, Plenum Press: New York, NY.
- [28] Kline, S. R. (2006). *J. Appl. Crystallogr.*, 39, 895–900.
- [29] Lagerwall, J. P. F., & Scalia, G. (2012). *Curr. Appl. Phys.*, 12, 1387–1412.
- [30] Nesrullajev, A., Okcan, M., & Kazanci, N. (2003). *J. Mol. Liq.*, 108, 313–332.
- [31] Bartolino, R., Chiaranza, T., & Meuti, M. (1982). *Phy. Rev. A.*, 26, 1116–1119.
- [32] Svergun, D. (1999). *Biophys. J.*, 76, 2879–2886.
- [33] Eastoe, J. et al. (2005). *J. Am. Chem. Soc.*, 127, 7302–7303.
- [34] Li, C. et al. (2010). *J. Colloid Interface Sci.*, 342, 354–360.
- [35] Zourab, S. M., & El-Samak, R. F. (2004). *J. Disper. Sci. Technol.*, 25, 41–51.